Journal of Medicinal Chemistry

ARTICLE

pubs.acs.org/jmc

Utilization of Nitrophenylphosphates and Oxime-Based Ligation for the Development of Nanomolar Affinity Inhibitors of the *Yersinia pestis* Outer Protein H (YopH) Phosphatase[†,‡]

Medhanit Bahta,[§] George T. Lountos,[∥] Beverly Dyas,[⊥] Sung-Eun Kim,[§] Robert G. Ulrich,[⊥] David S. Waugh,[∥] and Terrence R. Burke, Jr.*[,§]

[§]Chemical Biology Laboratory, Molecular Discovery Program, Center for Cancer Research, National Cancer Institute, National Institutes of Health, NCI—Frederick, Frederick, Maryland 21702, United States

[∥]Macromolecular Crystallography Laboratory, Center for Cancer Research, National Cancer Institute, National Institutes of Health, NCI—Frederick, Frederick, Maryland 21702, United States

[⊥]Laboratory of Molecular Immunology, United States Army Medical Research Institute of Infectious Diseases, Frederick, Maryland 21702, United States

Supporting Information

ABSTRACT: Our current study reports the first K_M optimization of a library of nitrophenylphosphate-containing substrates for generating an inhibitor lead against the *Yersinia pestis* outer protein phosphatase (YopH). A high activity substrate identified by this method (K_M = 80 μM) was converted from a substrate into an inhibitor by replacement of its phosphate group with difluoromethylphosphonic acid and by attachment of an aminooxy handle for further structural optimization by oxime ligation. A cocrystal structure of this aminooxy-containing platform in complex with YopH allowed the identification of a conserved water molecule proximal to the aminooxy group that was subsequently employed for the design of furanyl-based oxime derivatives. By this process, a potent (IC_{50} = 190 nM) and nonpromiscuous inhibitor was developed with good YopH selectivity relative to a panel of phosphatases. The inhibitor showed significant inhibition of intracellular *Y. pestis* replication at a noncytotoxic concentration. The current work presents general approaches to PTP inhibitor development that may be useful beyond YopH.

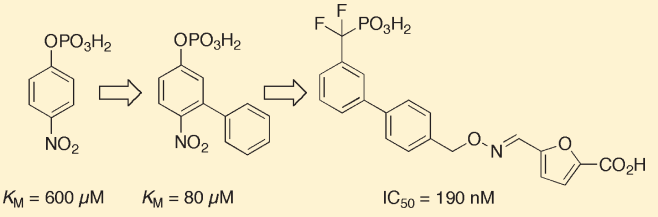

INTRODUCTION

Maintaining proper levels of tyrosyl phosphorylation through the reversible actions of protein tyrosine kinases (PTKs) and protein tryrosine phosphatases (PTPs) is vital for cellular processes ranging from growth and metabolism to adhesion and differentiation.[1,2] Deregulation of PTPs can be linked to diseases such as diabetes and cancer, and accordingly, this class of enzymes represents a new source of potential drug targets.[3−6] The Gram-negative enterobacterium *Yersinia pestis* (*Y. pestis*) has played an important role in human history as the causative agent of plague,[7] and more recently it has gained attention because of its possible use as a biological warfare agent. For pathogenicity, *Y. pestis* requires the virulence factor *Yersinia pestis* outer protein H "YopH", a highly active PTP.[8] Accordingly, potent and selective YopH inhibitors could provide a basis for new antiplague therapeutics. One difficulty encountered in the development of PTP inhibitors is a high incidence of "false positives" that can arise through inhibition of enzyme function by "promiscuous" mechanisms attributable to nonspecific factors such as protein aggregation.[9,10] It is generally believed that promiscuous inhibitors do not represent valid leads, and avoiding promiscuous mechanisms is an important component of current drug development.[11]

In theory, avoiding promiscuous behavior could be achieved through the use of substrates as templates for inhibitor design. This is because substrates must interact with their enzyme hosts in nonpromiscuous fashions in order for productive catalysis to occur. Employing small nonpeptidic arylphosphates to identify potential leads for PTP inhibitor design has been known for some time.[12−15] However, the explicit application of "substrate activity screening" for the purpose of minimizing misleading promiscuous inhibition has only more recently been proposed by Ellman for protease[16−20] and PTP targets.[21] This approach consists of first identifying substrates that exhibit high affinity, structurally enhancing these substrates, and then converting the optimized substrates to inhibitors by replacement of their labile phosphoryl groups with suitable nonhydrolyzable phosphoryl mimetics. Additional structural variations can then be performed to further increase inhibitory potency.

In the identification of high affinity substrates for the development of PTP inhibitors, advantage can be taken of the hydrolytic action of a PTP on an arylphosphate, which produces

Received: January 10, 2011
Published: March 28, 2011

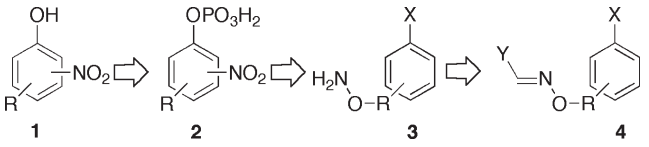

Figure 1. Design progression leading from a library of nitrophenylphosphates (**1**) to bidentate inhibitors (**4**).

both the corresponding phenol and inorganic phosphate. Traditionally, the released inorganic phosphate can be quantified using colorimetric assays that employ phosphomolybdate[22,23] or by secondary enzyme assays, including the use of purine nucleotide phosphorylase-mediated phosphate-dependent conversion of 2-amino-6-mercapto-7-methylpurine ribonucleoside to a derivative having an absorbance maximum at 360 nm.[24] It is also possible to spectrophotometrically measure the catalytically produced phenol. A variety of easily detected fluorescence-based substrates are known;[25] however, these agents would be of little value for the purpose of substrate activity screening and phenols derived from the more structurally diverse arylphosphates needed for substrate activity screening would typically exhibit very low extinction coefficients.[26] An exception to this is found with nitrophenols, which exhibit intense yellow color because of delocalization of the phenolate anionic charge. Because of this property, *p*-nitrophenylphosphate (*p*NPP) has become a ubiquitous substrate for monitoring the activity of phosphatases, including YopH.[8]

In undertaking our current study, we desired to use direct spectrophotometric monitoring of phenol reaction products. For this purpose, we employed substrates (**2**) derived from either *o*- or *p*-nitrophenols (**1**, Figure 1). These compounds allowed the simple monitoring (absorbance at λ_{405} nm) of yellow color resulting from the enzyme-catalyzed phosphoryl hydrolysis. Our utilization of nitrophenylphosphates represents the first systematic application of this structural class for PTP substrate optimization.

Once an inhibitor platform has been identified through a substrate activity approach, enhancement of affinity can be undertaken by introducing additional functionality intended to interact with sites proximal to the catalytic cavity.[27−33] A distinctive feature of the methodology in our current report is its incorporation of aminooxy functionality into the lead inhibitor platform (**3**) and the use of this handle for oxime-based derivatization (**4**, Figure 1). Functional group ligation by means of oxime bond formation can be considered to be a form of "click chemistry"[34] that we[35−38] and others[39−42] have shown can be highly useful for the facile generation of compound libraries. In the case of PTPs, azide−alkyne Huisgen cycloaddition click reactions have been used previously for the rapid assembly of bidentate libraries targeting protein tyrosine phosphatase 1B (PTP1B) and *Mycobacterium* protein tyrosine phosphatase B (*m*PTPB).[43−45] However, a potential limitation of this type of click chemistry is the requirement for high throughput syntheses of azide-containing libraries of reactants.[46] In contrast, oxime-based click chemistry is advantageous because it can be conducted using commercially available aldehydes and reaction products can be directly evaluated biologically without purification. As reported in our current paper, nitrophenylphosphate-based substrate activity screening used in combination with oxime ligation proved to be highly a successful approach that resulted in the development of a nonpromiscuous YopH inhibitor exhibiting a nanomolar IC_{50}.

RESULTS AND DISCUSSION

Nitrophenylphosphate Substrates. A total of 48 *o*- and *p*-nitrophenylphosphate-containing substrates (**2**) were prepared by phosphorylation (reaction with $HPO_3(Bn)_2$) of either commercially available or synthetic nitrophenols, followed by TFA-mediated cleavage of the resulting benzyl protecting groups. The YopH affinities of these substrates were determined using an in vitro assay that measured substrate turnover by monitoring the yellow color arising from the reaction product nitrophenols.[8] Color interference arising from sources other than the nitrophenol products did not prove to be problematic. Assay results for a subset of 11 selected substrates (**2a**−**k**, Table 1) show that the 3-aminooxymethyl-containing substrate **2e** exhibited a 3.5-fold decrease in its Michaelis−Menten constant (K_M = 170 μM) relative to *p*NPP (K_M = 600 μM) while *p*-phenyl-*o*-nitrophenylphosphate (**2j**) showed an approximate 4-fold decrease in its K_M (150 μM). The lowest K_M was obtained with *m*-phenyl-*p*-nitrophenylphosphate (**2k**, K_M = 80 μM), which showed an approximate 7.5-fold decrease relative to reference *p*NPP.

Lead Inhibitor Platform 5. When substrates are used as structural models for inhibitor design, the interpretation of data from the substrate enzyme assays can be an important factor. In the current study, K_M values were used to indicate substrate affinity. Previous comparisons of K_M and k_{cat}/K_M for small-molecule non-peptidyl aryl substrates have shown that K_M values more closely reflect IC_{50} and K_i than do k_{cat}/K_M ratios.[12−14,21] On the basis of this consideration, substrate **2k** was selected for conversion to an inhibitor because of its low K_M.

In the conversion of a PTP substrate to an inhibitor, the choice of phosphoryl mimetic can have a dramatic effect on the resulting inhibitory potency.[21] In our current work α,α-difluoromethylphosphonic acid[47] was used as a phosphoryl replacement, since it is isosteric with the parent phosphate group and it has been shown to be one of the highest affinity phosphoryl replacements in PTP contexts (Scheme 1).[48,49] A further consideration deals with the fate of the nitro functionality, since its role as a chromophore is no longer needed. Although an example has been reported where protein hydrogen bonding exists for the nitro group of a YopH-bound inhibitor,[50] in the current work the nitro functionality was removed at this stage. The transformation of **2k** to the inhibitor platform **5** was completed by introduction of an aminooxy handle for use in preparing bidentate inhibitors (**6**) using oxime-based click chemistry (Figure 2).[34−42]

Synthesis of Aminooxy-Containing Platform 5. The synthesis of **5** began with the CuBr and zinc promoted coupling reaction of diethyl (bromodifluoromethyl)phosphonate with 3-iodobromobenzene[51] to give the corresponding (difluoromethyl) phosphonic acid diethyl ester product **7** (Scheme 1). Suzuki coupling of **7** with 4-hydroxymethylboronic acid to give the biphenyl product **8** was followed by Mitsunobu reaction with *N*-hydroxyphthalimide and treatment of the resulting phthalimide with hydrazine hydrate to yield the aminooxy-containing diethylphosphonate **9** (79% yield). Finally, conversion of **9** to platform **5** was achieved through TMSBr-mediated phosphonate deprotection (Scheme 1).[52]

Crystal Structure of YopH in Complex with Platform 5. In order to facilitate inhibitor optimization, the X-ray cocrystal structure of **5** bound to YopH was determined. The orientation of the phosphonodifluormethyl group of **5** within the catalytic pocket was observed to be highly similar to that previously reported for the phosphonodifluormethylphenylalanyl residue

Table 1. In Vitro YopH K_M for Selected Substrates

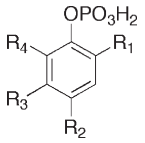

substrate	R_1	R_2	R_3	R_4	$K_M \pm$ SE (mM)[a]
*p*NPP	H	NO_2	H	H	0.60 ± 0.10
2a	NO_2	*t*-Bu	H	H	0.47 ± 0.06
2b	H	NO_2	*t*-Bu	H	1.14 ± 0.19
2c	NO_2	$-CH_2ONH_2$	H	H	1.13 ± 0.15
2d	H	NO_2	$-CH_2ONH_2$	H	0.41 ± 0.05
2e	H	NO_2	$CH_2ON{=}CHMe$	H	0.17 ± 0.02
2f	H	NO_2	H	Me	0.65 ± 0.11
2g	NO_2	H	H	Me	no activity
2h	cyclohexyl	NO_2	H	H	0.26 ± 0.02
2i	NO_2	H	H	cyclohexyl	no activity
2j	NO_2	Ph	H	H	0.15 ± 0.03
2k	H	NO_2	Ph	−H	0.08 ± 0.01

[a] K_M values were determined as indicated in the Materials and Methods.

Scheme 1. Synthesis of Inhibitor Platform 5[a]

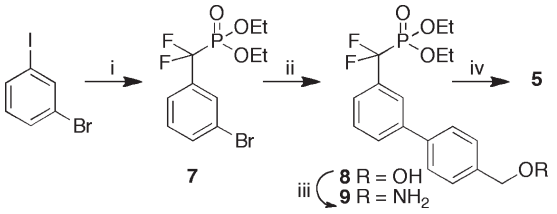

[a] Reagents and conditions: (i) Zn, diethyl (bromodifluoromethyl)-phosphonate, CuBr, DMF, 60 °C to room temperature (96% yield); (ii) 4-(hydroxymethyl)phenylboronic acid, $Pd(PPh_3)_4$, sat. K_2CO_3, EtOH, PhMe, 70 °C (45% yield); (iii) (a) *N*-hydroxyphthalimide, PPh_3, DIAD, THF, room temperature; (b) $NH_2NH_2 \cdot H_2O$, EtOH, room temperature (75% yield); (iv) TMSBr, CH_2Cl_2, room temperature (72% yield).

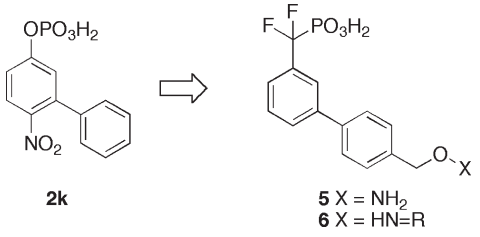

Figure 2. Development of oxime-containing inhibitors (**6**) starting from platform **2k**.

(F_2Pmp) of the hexapeptide Ac-Asp-Ala-Asp-Glu-F_2Pmp-Leu-amide (PDB code 1QZ0) (Figure 3A).[53] The protein backbones of the two structures are nearly superimposable, and in both structures the flexible "WPD loops" (residues 354−356) are held in the "closed" conformation. For both structures the phosphoryl-mimicking difluoromethylphosphonic acid group is coordinated within the conserved (H/V)CX5R(S/T) signature motif "P loop" (residues 404−410) by six hydrogen bonds,[54−56] while the guanidine group of R409 forms two salt bridges with two phosphonic acid oxygen atoms and indirect hydrogen bonds with residues Q357, Q450, and Q446 are made through a conserved water residue (designated as "Wa1" for ligand **5** and "cw" in PDB 1QZ0). The 1-phenyl ring of **5** is pivoted about the difluoromethylene carbon so that it is offset, yet within the same plane relative to the F_2Pmp aryl ring in the 1QZ0 structure. This allows the 3-(4′-methylphenyl) moiety of **5** to interact, similar to the Leu side chain of the dipeptide unit F_2Pmp-Leu in the 1QZ0 structure (Figure 3A). The aryl rings of **5** form extensive hydrophobic contacts with residues F229, D231, I232, A405, Q446, and I443, similar to what is observed in the 1QZ0 structure (Figure 3 and Table 2).

Introduction of Oxime Functionality into 5. In the cocrystal structure the aminooxyamine of **5** forms hydrogen bonds with the side chain carboxyl of D231 and a water molecule (Wa43), which also hydrogen-bonds to the D231 residue (Figure 4A). The importance of this latter water is indicated by its presence in the absence of inhibitor (designated as "Wa87" in PBD code 1LYV), suggesting that it could be used for inhibitor design. In silico docking studies performed using the cocrystal structure of **5** with the inclusion of Wa43[57,58] identified furanyl-based oximes as providing favorable interactions with the D231 residue through the intermediacy of the conserved water (Figure 4B).

Syntheses of a series of furanyl-based oxime inhibitors was performed in DMSO by reacting **5** (24 mM) with commercially available furanyl aldehydes and AcOH in the ratio (1:1:2). The oxime products (**6**), which were typically of >90% purity as shown by random HPLC analysis, were used directly for biological evaluation. Inhibitory potencies (IC_{50}) were obtained spectrophotometrically in an in vitro YopH assay using *p*NPP as substrate.[38]

The 3-furanyloxime (**6a**) showed an IC_{50} of 3.69 μM, whereas the 2-furanyloxime (**6b**) was approximately 3-fold more potent (IC_{50} = 1.20 μM) (Table 3). In modeling studies, the furanyl oxygen in **6a**

dx.doi.org/10.1021/jm200022g | J. Med. Chem. 2011, 54, 2933–2943

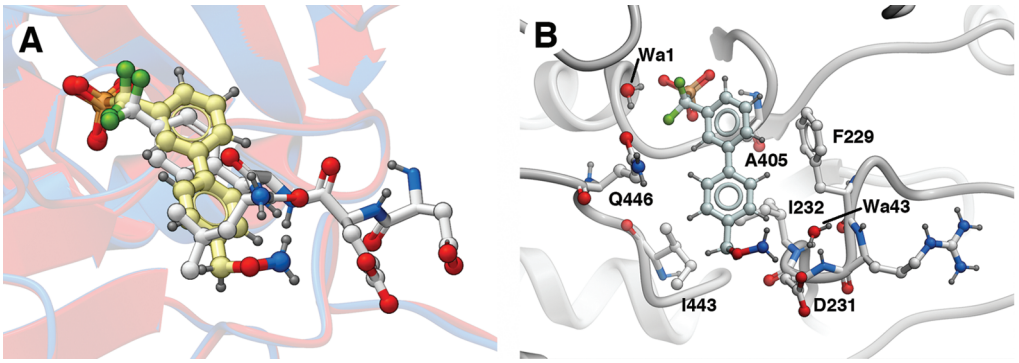

Figure 3. Crystal structures of YopH-bound ligands. (A) Superposition of the complex YopH−[Ac-Asp-Ala-Asp-Glu-F_2Pmp-Leu-amide] (protein backbone in red, ligand carbons in white; PDB code 1QZ0) with YopH−**5** (protein backbone in blue, ligand carbons in yellow) showing relative binding orientations of the two ligands. (B) Residues providing key hydrophobic contacts with **5**.

Table 2. Comparison of YopH Hydrophobic Contact Residues for Compound 5 and F_2Pmp-Leu

residue	**5**[a]	F_2Pmp-Leu[a,b]
F229	24.6	24.6
D231	24.1	30.2
I232	23.6	19.8
A405	23.0	24.1
Q446	21.1	29.1
I443	11.0	16.0

[a] Contact is given in Å^2. [b] Data for F_2Pmp-Leu was derived from PDB code 1QZ0.

was seen to be at a greater distance from the conserved Wa43 than for **6b**. Therefore, **6b** was modified by sequential addition of a 5-methyl group (**6c**, IC_{50} = 0.91 μM) and then by introduction of a hydroxyl group onto this methyl (**6d**, IC_{50} = 0.73 μM) and finally by oxidation of the 5-hydroxymethyl substitutent to a carboxyl group (**6e**, IC_{50} = 0.19 μM). This sequence of modifications resulted in a 6-fold improvement relative to the parent **6b**. The observed binding enhancement of **6e** was consistent with in silico docking studies that showed multiple interactions of its carboxyfuranyl oxime with the conserved Wa43 and with the backbone amide proton of R230 (Figure 4C).

Examination of Specificity of 6e. The development of YopH inhibitors is less advanced than for several other phosphatases. For example, while the literature contains numerous reports of nanomolar-affinity PTP1B inhibitors,[59] there are few examples of YopH inhibitors exhibiting affinities in the submicromolar range.[30,60] Additionally, the development of PTP inhibitors is plagued by a high incidence of false positives that are due to nonspecific or promiscuous mechanisms arising from the formation of colloid protein aggregates,[9,10,61,62] and for some YopH inhibitors the possible roles of promiscuous mechanisms are unclear. The nanomolar IC_{50} of **6e** makes it one of the more potent YopH inhibitors reported to date. In order to determine whether promiscuous mechanisms are at work, assays were conducted in the presence and absence of 0.01% TX-100, since it is known that promiscuous inhibition can often be minimized by the addition of such a detergent.[62] These experiments showed that the inhibitory potency of **6e** is independent of detergent concentration, providing strong evidence that YopH inhibition by **6e** does not arise through promiscuous mechanisms.

It was also of interest to examine possible YopH selectivity of **6e**, since significant structural homology exists among many phosphases. For this purpose, the inhibitory activity of **6e** was measured against a panel of phosphatases that included the classical tyrosine-specific phosphatases PTP1B and leukocyte antigen related phosphatase (LAR),[63] as well as the dual specificity phosphatases 14 and 22[64] (DUSP14, DUSP22) and the Variola phosphatase VH1. In these assays **6e** showed an approximate 17-fold selectivity for YopH relative to PTP1B and greater than 2000-fold selectivity relative to the other phosphatases examined (Table 4).

Evaluation of 6e in Biological Models. A cell-based assay was used to assess toxicity of **6e**. The mouse macrophage line J774 was cultured 40 h with 0.1−100 μM **6e**, and toxicity was measured by cellular ATP content. No toxicity for any compound was observed for **6e** below100 μM (data not shown). Intracellular replication of *Y. pestis* was assessed by a previously described human monocyte infection model.[65] Primary human monocytes were infected for 12 h with *Y. pestis*, using cell culture media containing 0.1−100 μM inhibitors or control. Specific inhibition of intracellular bacterial growth was observed with 10 μM **6e** (Figure 5). An approximately 9-fold decrease in intracellular bacteria resulted from treatment with **6e** compared to a negative control that showed no inhibition of YopH. The positive control gentamycin (10 μM), which targets bacterial ribosomes,[66] produced nearly complete inhibition of intracellular *Y. pestis* growth.

CONCLUSIONS

YopH has proven to be a difficult target for inhibitor development. While there are numerous reports of nanomolar affinity inhibitors against other phosphatases such as PTP1B, submicromolar affinity YopH inhibitors are very few. The current study represents the first utilization of a library of nitrophenylphosphate-containing substrates for the purposes of lead identification. An attractive feature of this approach is that K_M can be calculated directly by colorimetric methods based on the enzymatic generation of nitrophenol chromophore-containing reaction products. The current work is also characterized by its use of oxime-based click ligation to optimize a substrate-derived lead. The combination of these two methodologies allowed the identification of a nonpromiscuous nanomolar affinity YopH inhibitor exhibiting good PTP selectivity that showed significant inhibition of intracellular *Y. pestis* replication at a noncytotoxic

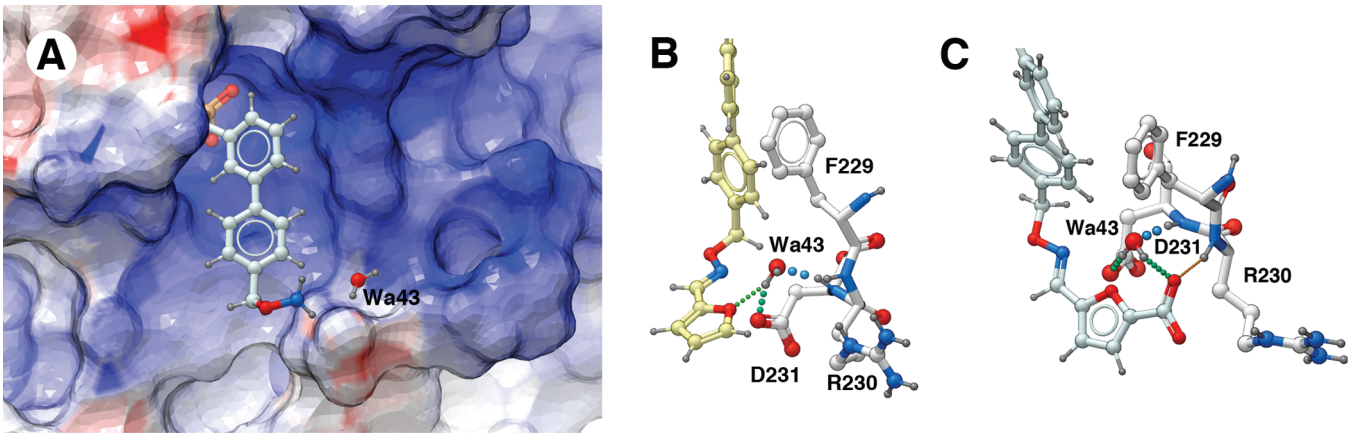

Figure 4. Role of conserved water (Wa43) in the design of inhibitor **6e**: (A) electrostatic potential surface rendering (blue = postive; red = negative) of the YopH−**5** complex highlighting a key conserved water (Wa43); (B) predicted interaction of the furanyloxime oxygen of **6b** with Wa43; (C) predicted interaction of the 5-carboxyfuranyloxime group of **6e** with Wa43 and the protein backbone.

concentration. The current work provides valuable insights into the development of YopH inhibitors that may have broader applicability in the discovery of inhibitors directed against other phosphatases.

MATERIALS AND METHODS

General. The following reagents used for YopH enzyme assays were obtained from Sigma-Aldrich: *p*NPP tablets, 30% BSA solution (protease free), 1.0 M HEPES solution (pH 7.0−7.6), and dithiotreitol (DTT). Aqueous ethylenediaminetetraacetic acid, sodium salt EDTA (0.5 M, pH 8.0) was obtained from Invitrogen, and 96-well plates were purchased from Costar. All reactions were carried out under argon unless otherwise stated. All solvents were anhydrous and obtained from Sigma-Aldrich. Final products were purified by a high pressure liquid chromatography (HPLC) using a Waters Prep-LC 4000 system and Phenomenex Gemini 10 μm, 110 Å C18 columns (250 mm × 21.20 mm, 10 μm) at a flow rate of 10 mL/min (preparative HPLC) with a mobile phase of A = 0.1% aqueous TFA and B = 0.1% TFA in aqueous acetonitrile. Typical gradients were from 10% B to 100% B over 40 min with UV monitoring at 220, 254, and 280 nm. The purity of final products was determined by analytical HPLC using a Waters Prep-LC 4000 system and Phenomenex Gemini 5 μm, 110 Å C18 columns (250 mm × 4.60 mm, 5 μm) at a flow rate of 1 mL/min with a mobile phase of A = 0.1% aqueous TFA and B = 0.1% TFA in aqueous acetonitrile. All final products were found to be ≥95% pure. NMR spectra were recorded using a Varian 400 MHz spectrometer. Unit mass resolution LC−MS results were obtained on synthetic intermediates, and high resolution mass spectra were obtained for final products (University of California at Riverside Mass Spectral Facility). Optical densities were measured with Biotek Synergy 2 spectrophotometer at λ_{abs} = 405 nm using a kinetic readout for determination of K_M and absolute readout for determination of IC_{50}. The PTPse domain of YopH (residues 164−468) was expressed in *Escherichia coli* according to a previously published procedure.[53]

Recombinant Proteins. The PTPase domain of YopH (residues 164−468) was expressed in *Escherichia coli* and purified as described previously,[8,53] as were the Variola major H1 (VH1)[67] and human DUSP-14 dual specificity phosphatases.[68] Human DUSP-22, PTP1B, and LAR catalytic domains were expressed and purified using generic methodology.[69]

Determination of YopH Michaelis−Menten Constants (K_M) for Nitrophenylphosphates. Total reactions volumes of 100 μL/well of reaction volume were used in 96-well plates. Buffer was prepared by mixing 25 mM Hepes buffer (pH 7.0−7.6), 50 mM NaCl, 2.5 mM EDTA, and 5 mM dithiothreitol (DTT) with 1 mM fresh DTT added right before an assay run. To each well was added 85 μL of assay buffer, 0.25% BSA (5 μL) followed by 5 μL of nitrophenylphosphate substrate in DMSO at dilutions of 1000, 500, 250, 125, 50, 25, 10, and 5 μM. To the reaction mixtures was then added 5 μL of YopH in buffer (25 μg/mL), and hydrolysis of substrate was monitored at 30 s intervals over 15 min. Michaelis−Menten constants (K_M) were determined using nonlinear regression with the equation $y = V_{max}[x/(K_M + x)]$. Values for *p*NPP and synthetic substrates **2a**−**k** are shown in Table 1. Data curves are provided in the Supporting Information.

Determination of YopH IC_{50} Values. Total reactions volumes of 100 μL/well of reaction volume were used in 96-well plates. Buffer was prepared as above. To each well was added 79 μL of assay buffer, 0.25% BSA (5 μL) followed by 5 μL of inhibitors in DMSO at dilutions of 400, 133, 44, 15, 5, 1.67, 0.56, 0.19, 0.063, 0.032, and 0 μM. To the reaction mixtures was then added 5 μL of YopH in buffer (25 μg/mL) followed by 6 μL of 10 mM *p*NPP buffer, and each plate was agitated gently at 25 °C for 15−20 min. Hydrolysis of the substrate was immediately measured. IC_{50} values were determined by fitting the data with a sigmoidal curve generated using the Boltzman equation. A parallel independent assay was performed with 0.01% TritonX-100. Inhibition constants for **6a**−**e** are provided in Table 3. Data curves are provided in the Supporting Information.

Toxicity Assay. Toxicity of **6e** was assessed with the mouse macrophage line J774 (American Type Culture Collection, Manassas, VA), cultured in Eagle's minimum essential medium supplemented with 4 mM L-glutamine, 4500 mg/L glucose, 1500 mg/L sodium bicarbonate, and 7.5% fetal bovine serum (GIBCO/Invitrogen, Carlsbad, CA). Cells were grown in 96-well (5×10^5 cells/100 mL) polystyrene plates (opaque bottom; Corning, Lowell, MA), maintained in a 5% CO_2, humid air incubator (37 °C). Inhibitor **6e** was dissolved in DMSO to produce a 10 mM stock solution and then added to cultures by diluting in media to final concentrations of 0.1−100 μM. A negative control was also used that shows no inhibition of YopH. Culture media for all cells contained a final 1% DMSO, including control wells without chemical compounds. Cell viability was assessed by ATP content 20 and 40 h after treatment, using a commercial kit (ViaLight, Lonza, Basel, Switzerland) and a luminometer (Wallac 1420 Victor; PerkinElmer, Shelton, CT) to measure photon emission.

Intracellular Replication of Bacteria. Primary human monocyte cultures[65] were used to measure intracellular replication of the plague bacterium. The *Y. pestis* strain CO92 *pgm*−, *pla*−, was previously described.[70] Colony-isolated bacteria were grown for 12 h in heart-infusion

dx.doi.org/10.1021/jm200022g |*J. Med. Chem.* 2011, 54, 2933–2943

Table 3. In Vitro YopH IC_{50} for Selected Inhibitors

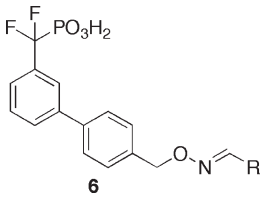

6

No.	R	IC_{50} ± S.E. (μM)[a]
6a		3.69 ± 0.31
6b		1.20 ± 0.22
6c	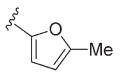	0.91 ± 0.13
6d	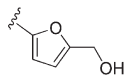	0.73 ± 0.30
6e	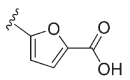	0.19 ± 0.16

[a] IC_{50} values were determined as indicated in Materials and Methods.

Table 4. Inhibitory Potencies of 6e against a Panel of Phosphatases[a]

phosphatase	IC_{50} (μM)	fold difference
YopH	0.19	ref value
PTP1B	2.23	11.7
LAR	>400	>2000
DUSP-14	>400	>2000
DUSP-22	>400	>2000
VH1	>400	>2000

[a] Values were determined as described in Materials and Methods.

broth (HIB; Difco Laboratories, Detroit, MI) supplemented with 0.2% xylose and 2.5 mM $CaCl_2$. A dilution of the culture was grown (26 °C) to mid-log phase, and the bacteria were pelleted by centrifugation (600*g*) before rinsing with RPMI 1640 medium. Human peripheral blood monocytes (CD14+) were isolated as previously described[65] and added (2×10^5/well) to tissue culture plates (96-well, flat bottom; Corning) in 100 μL of RPMI 1640 supplemented with 5% human AB sera (Life Technologies, Carlsbad, CA). The monocytes were incubated (1 h, 37 °C) with a 1:1 ratio of *Y. pestis* in a 5% CO_2, humid air incubator (37 °C). The wells were pulsed with gentamycin (10 μg/mL, 20 min) and rinsed with warm media to remove remaining extracellular bacteria. The cells were then cultured for 12 h in a 5% CO_2, humid air incubator (37 °C) in media (100 μL of RPMI 1640 supplemented with 5% human AB sera) containing 0.1−100 μM **6e** or a negative control that shows no inhibition of YopH. As a positive control, gentamycin was added to wells containing no other inhibitors. All cultures contained 1% DMSO by volume. The wells were then gently washed with warm medium, followed by addition of 120 μL of sterile distilled water to lyse the cells. The cell lysates were serially diluted (1:5) in HIB, and 200 mL of each dilution was placed into duplicate wells of a culture plate (Honeycomb; Growth Curves USA, Piscataway, NJ) and placed in a growth-monitoring incubator (Bioscreen; Growth Curves USA) with constant agitation (37 °C). Bacterial growth was measured by optical density at 600 nm every 20 min for 16 h. The amount of *Y. pestis* was quantified by comparison to a standard curve of bacteria.

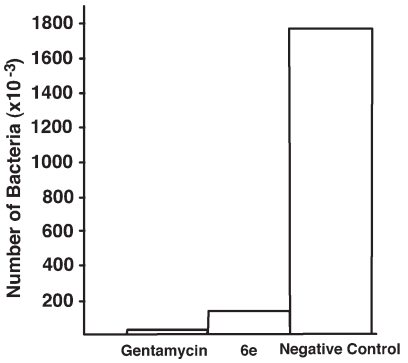

Figure 5. Effect of compounds on intracellular replication of *Y. pestis*. Primary human monocytes were infected with *Y. pestis* and cultured for 12 h with **6e** or a negative control (10 μM each). Gentamycin was included as a positive control. Results are presented as viable intracellular bacteria recovered per well of monocytes. Standard errors of the mean were <10%. The assay was performed on three separate occasions using three independent monocyte donors.

X-ray Crystallography. The purified protein was pooled and concentrated by diafiltration to 17.6 mg/mL in 100 mM sodium acetate, pH 5.7, 100 mM NaCl, and 1 mM EDTA. Crystals of YopH were obtained with condition D8 (0.1 M buffer system 2, pH 7.5, 0.12 M alcohols, 12.5% v/v MPD, 12.5% w/v PEG 1000, and 12.5% w/v PEG 3350) from the Molecular Dimensions (Apopka, FL) Morpheus screen.[71] A 1:1 ratio of protein (17.6 mg/mL) to well solution was used for crystallization at room temperature. Platelike crystals grew within 3 days. To obtain the protein−inhibitor complex, compound **5** was dissolved in DMSO and added to the crystallization solution to obtain a final concentration of 10 mM (10% DMSO). The crystals were added to the soaking solution and soaked for 48 h at room temperature. Crystals were flash-frozen in liquid nitrogen without the need of an additional cryoprotectant.

X-ray diffraction data for the YopH−**5** complex were collected at beamline 22-ID of the SER-CAT facilities at the Argonne National Laboratory utilizing remote data collection. By use of 1.0 Å X-ray wavelength, 180 frames of data were collected using an exposure time of 3 s and oscillation angle of 1°. The X-ray diffraction data were processed with HKL3000.[72] Data collection and refinement statistics are outlined in Table 5. The structure was solved by molecular replacement using the MOLREP program[73] from the CCP4 suite[74] and the coordinates of the previously solved YopH structure (PDB code 1QZ0)

Table 5. Data Collection and Refinement Statistics

parameter	
X-ray source	22-ID, SER-CAT
wavelength (Å)	1.0
resolution (Å)	50.0−1.78 (1.80−1.78)[a]
space group	$P\,2_12_12_1$
unit cell dimensions	
a (Å)	49.2
b (Å)	55.5
c (Å)	100.1
total reflections/unique reflections	148922/25241
completeness (%)	92.8/74.8
R_{sym} (%)[b]	10.6 (49.8)
$I/\sigma(I)$	21.9 (2.3)
redundancy	5.9 (4.1)
refinement statistics[c]	
resolution (Å)	50.0−1.78
no. of reflections working set/test set	23875/25241
R_{work} (%)	16.5
R_{free} (%)	21.0
no. of atoms, mean *B*-factor (Å^2)	
protein	2237/15.5
inhibitor	22/15.7
water	274/29.3
rms deviation from ideal geometry	
bond length (Å)/bond angle (deg)	0.014/1.5
Ramachandran plot	
most favored (%)	93.2
additionally allowed (%)	6.4
generously allowed (%)	0.4
disallowed (%)	0
MolProbity protein geometry score	1.53 (92nd percentile)
PDB accession code	2Y2F

[a] Values in parentheses are for reflections in the highest resolution shell. [b] $R_{sym} = \Sigma_{hkl}\Sigma_i|I_i(hkl) - \langle I(hkl)\rangle|/\Sigma_{hkl}\Sigma_i I_i(hkl)$, where $\langle I(hkl)\rangle$ is the mean intensity of multiply recorded reflections. [c] $R = \Sigma|F_{obs}(hkl) - F_{calc}(hkl)|/\Sigma\,|F_{obs}(hkl)|$. R_{free} is the *R* calculated for 5% of the data set not included in the refinement.

after removing all solvent and ligand atoms. Cross-rotation and translational searches were performed using data up to 3.0 Å followed by rigid-body refinement with REFMAC5.[75] Iterative rounds of model rebuilding and refinement were performed with COOT[76] and REFMAC5, and the location of the inhibitor was unambiguously identified using σ_A-weighted $2mF_o - DF_c$ and $mF_o - DF_c$ electron density maps.[77] The coordinates and refinement restraint files were prepared using the Dundee PRODRG server.[78] Water molecules were located using COOT and refined with REFMAC5. The refinement was monitored by setting aside 5% of the reflections for calculation of the R_{free} value.[79] Model validation was performed using MolProbity.[80] The electron density map for YopH-bound inhibitor **5** is included in the Supporting Information. The coordinates and structure factor files were deposited in the Protein Data Bank with accession code 2Y2F.

In Silico Studies. Docking of inhibitors **6a** and **6e** onto YopH was done with ICM Chemist Pro software[57] running on a MacIntosh computer (OSX, version 10.5.8) using default parameters and procedures.[58] In summary, modeling started with the X-ray crystal structure of YopH in complex with **5**. The "convert PDB" command was used to convert to native ICM format, with optimization of hydrogens. All H_2O molecules were removed from the enzyme with the exception of the catalytically conserved water (Wa1) and a conserved water proximal to the ligand aminooxy group (Wa43) (see Figure 4A). A 2-furanyl-based oxime group was added to the aminooxyamine of **5**, and the resulting oxime structure (**6a**) was redocked using the "re-dock" option under the "Ligand" menu (see Figure 4B). All docking experiments were performed using the standard "re-dock" command, which utilizes a rigid receptor protocol. The docked **6a** was then modified by addition of a carboxyl group to the furanyl 5-position, and the resulting structure (**6e**) was redocked as described above (see Figure 4C).

General Procedure for the Synthesis of Nitrophenylphosphate Substrates (2a−k). To a solution of *o*- or *p*-nitrophenol (1.0 mmol) in CH_2Cl_2 (5 mL) was added CCl_4 (5.0 mmol) at −15 °C, and the reaction mixture was stirred at −15 °C (5−10 min). To the mixture was added *N*,*N*-diisopropylethylamine (DIEA) (2.0 mmol) and *N*,*N*-dimethylaminopyridine (DMAP) (0.1 mmol). Then dibenzyl phosphite was added dropwise at −15 °C, and the mixture was stirred at −15 °C (1.5 h). The reaction was quenched by stirring with 0.5 M aqueous KH_2PO_4 (20 mL) at room temperature (5 min). The aqueous phase was extracted with EtOAc, and the combined organic extract was dried ($MgSO_4$) and taken to dryness under reduced pressure. The resulting residue was stirred with a solution of TFA/CH_2Cl_2 (1:1, 5 mL) for 2−3 h. Volatiles were removed by evaporation and crude products were subjected to HPLC purification to provide final products in yields of 75−100%.

4-(*tert*-Butyl)-2-nitrophenyl Dihydrogen Phosphate (2a). ^{1}H NMR (400 MHz, CD_3OD): δ 7.86 (d, J = 2.0 Hz, 1H), 7.67 (dd, J = 2.4 Hz, J = 8.8 Hz, 1H), 7.44 (d, J = 8.8 Hz, 1H), 1.31 (s, 9H). ^{13}C NMR (400 MHz, CD_3OD): δ 149.99 (1C), 143.19 (1C), 143.04 (1C), 132.27 (1C), 123.66 (1C), 123.06 (1C), 35.69 (1C), 31.49 (3C). HRMS-ESI (m/z): $[M - H]^-$ calcd for $C_{10}H_{14}NO_6P$, 274.0486; found, 274.0490.

3-(*tert*-Butyl)-4-nitrophenyl Dihydrogen Phosphate (2b). ^{1}H NMR (400 MHz, CD_3OD): δ 7.42−7.46 (m, 2H), 7.18 (m, 1H), 1.39 (s, 9H). ^{13}C NMR (400 MHz, CD_3OD): δ 154.17 (1C), 149.26 (1C), 144.82 (1C), 126.89 (1C), 121.66 (1C), 119.79 (1C), 35.28 (1C), 29.36 (3C). HRMS-ESI (m/z): $[M - H]^-$ calcd for $C_{10}H_{14}NO_6P$, 274.0486; found, 274.0490.

4-((Aminooxy)methyl)-2-nitrophenyl Dihydrogen Phosphate (2c). ^{1}H NMR (400 MHz, D_2O): δ 8.09 (d, J = 2.2 Hz, 1H), 7.78 (dd, J = 2.4 Hz, J = 8.8 Hz, 1H), 7.59 (d, J = 8.8 Hz, 1H), 5.09 (s, 2H). HRMS-ESI (m/z): $[M - H]^-$ calcd for $C_7H_8N_2O_7P$, 263.0075; found, 263.0077.

3-((Aminooxy)methyl)-4-nitrophenyl Dihydrogen Phosphate (2d). ^{1}H NMR (400 MHz, D_2O): δ 8.27 (d, J = 9.2 Hz, 1H), 7.53 (s, 1H), 7.40 (d, J = 9.2 Hz, 1H), 5.41 (s, 2H). HRMS-ESI (m/z): $[M - H]^-$ calcd for $C_7H_8N_2O_7P$, 263.0075; found, 263.0067.

(3-(((Ethylideneamino)oxy)methyl)-4-nitrophenyl Dihydrogen Phosphate (2e). ^{1}H NMR (400 MHz, CD_3OD): δ 8.16 (d, J = 9.2 Hz, 1H), 7.36 (m, 1H), 7.27 (m, 1H), 6.98 (q, J = 5.6 Hz, 1H), 5.40 (s, 2H), 1.88 (d, J = 5.6 Hz, 3H). HRMS-ESI (m/z): $[M + H]^+$ calcd for $C_9H_{12}N_2O_7P$, 291.0377; found, 291.0374.

2-Methyl-4-nitrophenyl Dihydrogen Phosphate (2f). ^{1}H NMR (400 MHz, CD_3OD): δ 8.06 (m, J = 4.0 Hz, 1H), 8.00 (dd, J = 4.0 Hz, J = 8.0 Hz, 1H), 7.42 (d, J = 8.0 Hz, 1H), 2.34 (s, 3H). ^{13}C NMR (400 MHz, CD_3OD): δ 156.26 (1C), 145.43 (1C), 132.75 (1C), 127.32 (1C), 123.68 (1C), 121.33 (1C), 16.65 (1C). HRMS-ESI (m/z): $[M - H]^-$ calcd for $C_7H_8NO_6P$, 232.0016; found, 232.0011.

2-Methyl-6-nitrophenyl Dihydrogen Phosphate (2g). ^{1}H NMR (400 MHz, CD_3OD): δ 7.67 (dd, J = 1.2 Hz, J = 8.0 Hz, 1H), 7.50 (d, J = 9.5 Hz, 1H), 7.20 (td, J = 1.2 Hz, J = 8.0 Hz, 1H), 2.41 (s, 3H). ^{13}C NMR (400 MHz, CD_3OD): δ 145.15 (1C), 143.43 (1C), 136.75 (1C), 135.56 (1C), 126.02 (1C), 124.10 (1C), 17.04 (1C). HRMS-ESI (m/z): $[M + H]^+$ calcd for $C_7H_8NO_6P$, 234.0162; found, 234.0160.

2-Cyclohexyl-4-nitrophenyl Dihydrogen Phosphate (2h). ^{1}H NMR (400 MHz, CD_3OD): δ 7.68 (dd, J = 1.6 Hz, J = 8.0 Hz, 1H),

7.61 (dd, J = 1.2 Hz, J = 8.0 Hz, 1H), 7.30 (td, J = 1.2 Hz, J = 8.0 Hz, 1H), 3.09 (m, 1H), 1.75−1.88 (m, 5H), 1.30−1.53 (m, 5H). ^{13}C NMR (400 MHz, CD_3OD): δ 155.29 (1C), 145.93 (1C), 141.78 (1C), 123.91 (1C), 123.41 (1C), 121.50 (1C), 38.59 (1C), 34.19 (2C), 27.90 (2C), 27.20 (1C). HRMS-ESI (m/z): $[M + H]^+$ calcd for $C_{12}H_{16}NO_6P$, 300.0642; found, 300.0642.

2-Cyclohexyl-6-nitrophenyl Dihydrogen Phosphate (2i). ^{1}H NMR (400 MHz, CD_3OD): δ 8.15 (m, 1H), 8.07 (dd, J = 2.8 Hz, J = 8.8 Hz, 1H), 7.52 (dd, J = 1.2 Hz, J = 8.8 Hz, 1H), 3.30 (m, 1H), 1.77−1.90 (m, 5H), 1.32−1.51 (m, 5H). ^{13}C NMR (400 MHz, CD_3OD): δ 145.11 (1C), 144.68 (1C), 142.13 (1C), 133.31 (1C), 126.30 (1C), 123.85 (1C), 38.10 (1C), 34.77 (2C), 27.89 (2C), 27.20 (1C). HRMS-ESI (m/z): $[M + H]^+$ calcd for $C_{12}H_{16}NO_6P$, 300.0642; found, 300.0642.

3-Nitro-[1,1′-biphenyl]-4-yl Dihydrogen Phosphate (2j). ^{1}H NMR (400 MHz, CD_3OD): δ 8.07 (dd, J = 0.8 Hz, J = 2.4 Hz, 1H), 7.85 (dd, J = 2.0 Hz, J = 8.4 Hz, 1H), 7.58−7.60 (m, 3H), 7.41−7.45 (m, 2H), 7.35 (m, 1H). ^{13}C NMR (400 MHz, CD_3OD): δ 155.48 (1C), 144.51 (1C), 139.62 (1C), 139.38 (1C), 130.29 (2C), 129.47 (1C), 128.01 (2C), 124.44 (1C), 124.41 (1C), 124.36 (1C). HRMS-ESI (m/z): $[M + H]^+$ calcd for $C_{12}H_{11}NO_6P$, 296.0319; found, 296.0315.

6-Nitro-[1,1′-biphenyl]-3-yl Dihydrogen Phosphate (2k). ^{1}H NMR (400 MHz, CD_3OD): δ 7.95 (d, J = 8.8 Hz, 1H), 7.40−7.43 (m, 3H), 7.34−7.38 (m, 2H), 7.30−7.32 (m, 3H). ^{13}C NMR (400 MHz, CD_3OD): δ 155.48 (1C), 146.76 (1C), 139.79 (1C), 138.63 (1C), 129.76 (2C), 129.49 (1C), 128.90 (2C), 127.35 (1C), 129.32 (1C), 120.89 (1C). HRMS-ESI (m/z): $[M + H]^+$ calcd for $C_{12}H_{11}NO_6P$, 296.0319; found, 296.0316.

Diethyl ((3-Bromophenyl)difluoromethyl)phosphonate (7). A suspended solution of Zn dust (1.27 g, 19.4 mmol) in 3 mL of DMF was purged with argon. To this solution diethyl (bromodifluoromethyl)phosphonate (3.4 mL, 19.4 mmol) in 2 mL of DMF was added dropwise by maintaining reaction temperature at 50−60 °C (reaction is exothermic). The reaction mixture was stirred at room temperature for over 3 h. CuBr (2.79 g, 19.4 mmol) was added, and the mixture was stirred for 30 min at room temperature. A solution of bromo-3-iodobenzene (2.00 g, 7.1 mmol) in 1 mL of DMF was added dropwise and was stirred for over 24 h at room temperature. Water (10 mL) and ether (10 mL) were added, and mixture was passed through Celite. The layers were separated, and the aqueous layer was extracted by ether. The organic extract was dried over $MgSO_4$, filtered, and solvent was removed. The crude material was purified via silica gel column chromatography (9:1 to 2:1 hexanes/EtOAc) to give pale yellow oil product (2.3 g, 96%). ^{1}H NMR (400 MHz, $CDCl_3$): δ 7.71 (s, 1H), 7.58 (m, 1H), 7.52 (m, 1H), 7.29 (m, 1H), 4.19 (m, 4H), 1.29 (m, 6H). ^{13}C NMR (400 MHz, $CDCl_3$): δ 133.86 (1C), 129.99 (1C), 129.97 (1C), 129.85 (1C), 129.25 (1C), 129.97 (1C), 122.40 (1C), 64.92 (1C), 64.85 (1C), 16.29 (1C), 16.24 (1C). APCI-MS (m/z): calcd for $C_{11}H_{14}BrF_2O_3P$, 342.0 and 344.0; found, 343.0 and 345.0 $[M + H]^+$.

Diethyl (Difluoro(4′-(hydroxymethyl)-[1,1′-biphenyl]-3-yl)methyl)phosphonate (8). A mixture of **7** (500.0 mg, 1.46 mmol), (4-(hydroxymethyl)phenyl)boronic acid (332.0 mg, 2.19 mmol), and $Pd(PPh_3)$ (84.0 mg, 0.07 mmol) in 5 mL of a saturated solution of K_2CO_3, 2 mL of EtOH, and 5 mL of toluene was purged with argon and stirred at 70 °C overnight. Water (20 mL) was added upon cooling. The aqueous layer was extracted by EtOAc, and organic extract was dried over $MgSO_4$, filtered. The solvent was removed under reduced pressure. Crude material was purified via silica gel chromatography (1.5:1 to 1:3 hexanes/EtOAc) to give **8** as a colorless oil (308 mg, 57% yield). ^{1}H NMR (400 MHz, $CDCl_3$): δ 7.83 (m, 1H), 7.79 (m, 1H), 7.58 (m, 3H), 7.52 (m, 1H), 7.43 (m, 2H), 4.71 (s, 2H), 4.21 (m, 4H), 2.42 (s, 1H), 1.31 (m, 6H). ^{13}C NMR (400 MHz, CDCl3): δ 141.15 (1C), 140.78 (1C), 139.12 (1C), 133.11 (1C), 132.98 (1C), 129.36 (1C), 128.90 (1C), 127.40 (2C), 127.16 (2C), 124.95 (1C), 124.73 (1C), 64.90 (1C), 64.83 (1C), 16.31 (1C), 16.26 (1C). ESI-MS (m/z): calcd for $C_{18}H_{21}F_2O_4P$, 370.11; found, 393.20 $[M + Na]^+$.

Diethyl ((4′-((Aminooxy)methyl)-[1,1′-biphenyl]-3-yl)difluoromethyl)phosphonate (9). To a mixture of **8** (184.0 mg, 0.50 mmol), N-hydroxyphthalimide (98.1 mg, 0.60 mmol), and PPh_3 (170.2 mg, 0.65 mmol) in anhydrous THF (5 mL) was added diisopropyl azodicarboxylate (DIAD) (0.13 mL, 0.65 mmol). The mixture was stirred at room temperature overnight. The reaction mixture was partitioned (H_2O/EtOAc), and the organic layer was dried over $MgSO_4$ and solvent was removed under reduced pressure. To a solution of the resultant product (168 mg, 0.33 mmol) in CH_2Cl_2 (5 mL) and ethanol was added 50% aqueous hydrazine hydrate (80 μL, 1.30 mmol). The mixture was stirred at room temperature for 4 h. The resulting precipitate was removed by filtration, and solvent was removed from the filtrate. The crude product was purified by silica column chromatography (50−100% EtOAc in hexanes) to yield **9** as an amorphous white solid (100 mg, 79% yield). ^{1}H NMR (400 MHz, CD_3OD): δ 7.81 (m, 2H), 7.59 (m, 4H), 7.46 (m, 2H), 4.73 (s, 2H), 4.20 (m, 4H), 1.30 (m, 6H). ^{13}C NMR (400 MHz, CD_3OD): δ 141.17 (1C), 139.31 (1C), 137.26 (1C), 132.90 (1C), 132.76 (1C), 129.29 (1C), 129.27 (1C), 128.63 (2C), 128.23 (1C), 126.64 (2C), 124.63 (1C), 124.24 (1C), 76.98 (1C), 65.14 (1C), 65.07 (1C), 15.27 (1C), 15.21 (1C). APCI-MS (m/z): calcd for $C_{18}H_{22}F_2NO_4P$, 385.13; found, 386.10 $[M + H]^+$.

((4′-((Aminooxy)methyl)-[1,1′-biphenyl]-3-yl)difluoromethyl) phosphonic Acid (5). To a solution of **9** (100 mg, 0.26 mmol) in anhydrous CH_2Cl_2 (5 mL) under argon was added trimethylsilyl bromide (0.13 mL, 0.93 mmol), and the mixture was stirred at room temperature for 3 h. Solvent was removed, and HPLC purification was performed as described in the general synthetic methods section (retention time of 15.6 min) to provide **5** as an amorphous white solid (44.4 mg, 52% yield). Analytical HPLC gave 99% purity. ^{1}H NMR (400 MHz, DMSO-d_6): δ 7.69−7.73 (m, 2H), 7.56 (m, 2H), 7.49 (m, 2H), 7.36 (m, 2H), 4.70 (s, 2H). HRMS-ESI (m/z): $[M + H]^+$ calcd for $C_{14}H_{15}NO_4F_2P$, 330.0701; found, 330.0694.

(*E*)-5-((((3′-(Difluoro(phosphono)methyl)-[1,1′-biphenyl]-4-yl)methoxy)imino)methyl)furan-2-carboxylic acid (6e). To a solution of **5** (8.2 mg, 0.025 mmol) and 5-formylfuran-2-carboxylic acid (4.2 mg, 0.030 mmol) in 2 mL of DMSO was added AcOH (2.9 μL, 0.050 mmol). The reaction mixture was agitated at room temperature overnight. Product was purified via HPLC with a retention time of 18.4 min to give a white solid product (7.8 mg, 69%). ^{1}H NMR (400 MHz, CD_3OD): δ 8.07 (s, 1H), 7.77 (s, 1H), 7.67 (d, J = 7.2 Hz, 1H), 7.56−7.59 (m, 2H), 7.41−7.52 (m, 5H), 7.22, 7.16 (d, J = 3.6 Hz, 1H), 7.18, 6.76 (d, J = 3.6 Hz, 1H), 5.26, 5.17 (s, 2H). ^{13}C NMR (400 MHz, CDCl3): δ 159.78 (1C), 150.55 (1C), 147.54 (1C), 145.59 (1C), 140.75 (1C), 139.89 (1C), 139.02 (1C), 136.89 (1C), 135.45 (1C), 128.55 (2C), 128.46 (1C), 128.44 (1C), 126.75 (1C), 126.66 (2C), 124.52 (1C), 118.78 (1C), 112.77 (1C), 76.01 (1C). HRMS-ESI (m/z): $[M - H]^-$ calcd for $C_{20}H_{16}F_2NO_7P$, 450.0560; found, 450.0562.

■ ASSOCIATED CONTENT

Supporting Information. Curves for determination of substrate YopH Michaelis−Menten constants (K_M); YopH inhibition curves for oxime-containing inhibitors **6a**−**e**; electron density map for YopH-bound inhibitor **5** and NMR spectra. This material is available free of charge via the Internet at http://pubs.acs.org.

Accession Codes

[†]Coordinates and structure factor files have been deposited in the Protein Data Bank with accession code 2Y2F.

■ AUTHOR INFORMATION

Corresponding Author

*Phone: (301) 846-5906. Fax: (301) 846-6033. E-mail: tburke@helix.nih.gov.

■ ACKNOWLEDGMENT

Appreciation is expressed to Afroz Sultana (LMI) for technical support and to Joseph Tropea and Scott Cherry (MCL) for assistance with the production of phosphatases. Electrospray mass spectrometry experiments were conducted on the LC/ESMS instrument maintained by the Biophysics Resource in the Structural Biophysics Laboratory, Center for Cancer Research, National Cancer Institute at Frederick. X-ray diffraction data were collected at the Southeast Regional Collaborative Access Team (SER-CAT) beamline 22-ID at the Advanced Photon Source, Argonne National Laboratory. Supporting institutions may be found at http://www.ser-cat.org/members.html. Use of the Advanced Photon Source was supported by the U.S. Department of Energy, Office of Science, Office of Basic Energy Sciences, under Contract No. W-31-109-Eng-38. This work was supported in part by the Intramural Research Program of the NIH, Center for Cancer Research, NCI—Frederick and the National Cancer Institute, National Institutes of Health, and the Joint Science and Technology Office of the Department of Defense. The content of this publication does not necessarily reflect the views or policies of the Department of Health and Human Services, nor does mention of trade names, commercial products, or organizations imply endorsement by the U.S. Government.

■ ABBREVIATIONS USED

Y. pestis, *Yersinia pestis*; YopH, *Yersinia pestis* outer protein H; PTP, protein tyrosine phosphatase; PTK, protein tyrosine kinase *p*NPP, *p*-nitrophenylphosphate; PTP1B, protein tyrosine phosphatase 1B; *m*PTPB, *Mycobacterium* protein tyrosine phosphatase B; TFA, trifluoroacetic acid; F_2Pmp, difluorophosphonomethylphenyl; LAR, leukocyte antigen related; DUSP 14, dual specificity phosphatase 14; DUSP 22, Dual specificity phosphatase 22; BSA, bovine serum albumin; HEPES, 4-(2-hydroxyethyl)-1-piperazineethanesulfonic acid; EDTA, ethylenediaminetetraacetic acid, sodium salt

■ ADDITIONAL NOTE

[‡] A preliminary account of this work has been reported: Bahta et al. Application of Substrate Activity Screening in the Development of Inhibitors of the *Yersinia pestis* Protein Tyrosine Phosphatase, YopH. Presented at the 238th National Meeting of the American Chemical Society, Washington, DC, August 16−20, 2009; MEDI-178.

■ REFERENCES

(1) Soulsby, M.; Bennett, A. M. Physiological signaling specificity by protein tyrosine phosphatases. *Physiology* **2009**, *24*, 281–289.

(2) Hunter, T. Tyrosine phosphorylation: thirty years and counting. *Curr. Opin. Cell Biol.* **2009**, *21*, 140–146.

(3) Zhang, Z.-Y.; Lee, S.-Y. PTP1B inhibitors as potential therapeutics in the treatment of type 2 diabetes and obesity. *Expert Opin. Invest. Drugs* **2003**, *12*, 223–233.

(4) Ostman, A.; Hellberg, C.; Bohmer, F. D. Protein-tyrosine phosphatases and cancer. *Nat. Rev. Cancer* **2006**, *6*, 307–320.

(5) Jiang, Z.-X.; Zhang, Z.-Y. Targeting PTPs with small molecule inhibitors in cancer treatment. *Cancer Metastasis Rev.* **2008**, *27*, 263–272.

(6) Vidovic, D.; Schurer, S. C. Knowledge-based characterization of similarity relationships in the human protein-tyrosine phosphatase family for rational inhibitor design. *J. Med. Chem.* **2009**, *52*, 6649–6659.

(7) Titball, R. W.; Leary, S. E. Plague. *Br. Med. Bull.* **1998**, *54*, 625–633.

(8) Zhang, Z. Y.; Clemens, J. C.; Schubert, H. L.; Stuckey, J. A.; Fischer, M. W.; Hume, D. M.; Saper, M. A.; Dixon, J. E. Expression, purification, and physicochemical characterization of a recombinant Yersinia protein tyrosine phosphatase. *J. Biol. Chem.* **1992**, *267*, 23759–23766.

(9) McGovern, S. L.; Caselli, E.; Grigorieff, N.; Shoichet, B. K. A common mechanism underlying promiscuous inhibitors from virtual and high-throughput screening. *J. Med. Chem.* **2002**, *45*, 1712–1722.

(10) McGovern, S. L.; Helfand, B. T.; Feng, B.; Shoichet, B. K. A specific mechanism of nonspecific inhibition. *J. Med. Chem.* **2003**, *46*, 4265–4272.

(11) Seidler, J.; McGovern, S. L.; Doman, T. N.; Shoichet, B. K. Identification and prediction of promiscuous aggregating inhibitors among known drugs. *J. Med. Chem.* **2003**, *46*, 4477–4486.

(12) Zhang, Z.-Y. Kinetic and mechanistic characterization of a mammalian protein-tyrosine phosphatase, PTP1. *J. Biol. Chem.* **1995**, *270*, 11199–11204.

(13) Montserat, J.; Chen, L.; Lawrence, D. S.; Zhang, Z.-Y. Potent low molecular weight substrates for protein-tyrosine phosphatase. *J. Biol. Chem.* **1996**, *271*, 7868–7872.

(14) Chen, L.; Montserat, J.; Lawrence, D. S.; Zhang, Z.-Y. VHR and PTP1 protein phosphatases exhibit remarkably different active site specificities toward low molecular weight nonpeptidic substrates. *Biochemistry* **1996**, *35*, 9349–9354.

(15) Taylor, S. D.; Kotoris, C. C.; Dinaut, A. N.; Wang, Q.; Ramachandran, C.; Huang, Z. Potent non-peptidyl inhibitors of protein tyrosine phosphatase 1B. *Bioor. Med. Chem.* **1998**, *6*, 1457–1468.

(16) Wood, W. J. L.; Patterson, A. W.; Tsuruoka, H.; Jain, R. K.; Ellman, J. A. Substrate activity screening: a fragment-based method for the rapid identification of nonpeptidic protease inhibitors. *J. Am. Chem. Soc.* **2005**, *127*, 15521–15527.

(17) Salisbury, C. M.; Ellman, J. A. Rapid identification of potent nonpeptidic serine protease inhibitors. *ChemBioChem* **2006**, *7*, 1034–1037.

(18) Patterson, A. W.; Wood, W. J. L.; Ellman, J. A. Substrate activity screening (SAS): a general procedure for the preparation and screening of a fragment-based non-peptidic protease substrate library for inhibitor discovery. *Nat. Protoc.* **2007**, *2*, 424–433.

(19) Inagaki, H.; Tsuruoka, H.; Hornsby, M.; Lesley, S. A.; Spraggon, G.; Ellman, J. A. Characterization and optimization of selective, nonpeptidic inhibitors of cathepsin S with an unprecedented binding mode. *J. Med. Chem.* **2007**, *50*, 2693–2699.

(20) Brak, K.; Doyle, P. S.; McKerrow, J. H.; Ellman, J. A. Identification of a new class of nonpeptidic inhibitors of cruzain. *J. Am. Chem. Soc.* **2008**, *130*, 6404–6410.

(21) Soellner, M. B.; Rawls, K. A.; Grundner, C.; Alber, T.; Ellman, J. A. Fragment-based substrate activity screening method for the identification of potent inhibitors of the *Mycobacterium tuberculosis* phosphatase PTPB. *J. Am. Chem. Soc.* **2007**, *129*, 9613–9615.

(22) Jenkins, W. T.; Marshall, M. M. A modified direct phosphate assay for studying ATPases. *Anal. Biochem.* **1984**, *141*, 155–160.

(23) Black, M. J.; Jones, M. E. Inorganic phosphate determination in the presence of a labile organic phosphate: assay for carbamyl phosphate phosphatase activity. *Anal. Biochem.* **1983**, *135*, 233–238.

(24) Webb, M. R. A continuous spectrophotometric assay for inorganic phosphate and for measuring phosphate release kinetics in biological systems. *Proc. Natl. Acad. Sci. U.S.A.* **1992**, *89*, 4884–487.

(25) Tautz, L.; Mustelin, T. Stategies for developing protein tyrosine phosphatase inhibitors. *Methods* **2007**, *42*, 250–260.

(26) Zhang, Z.-Y. Pre-steady-state and steady-state kinetic analysis of the low molecular weight phosphotyrosyl protein phosphatase from bovine heart. *J. Biol. Chem.* **1991**, *266*, 1516–1525.

(27) Puius, Y. A.; Zhao, Y.; Sullivan, M.; Lawrence, D. S.; Almo, S. C.; Zhang, Z.-Y. Identification of a second aryl phosphate-binding site in protein-tyrosine phosphatase 1B: a paradigm for inhibitor design. *Proc. Natl. Acad. Sci. U.S.A.* **1997**, *94*, 13420–13425.

(28) Guo, X.-L.; Shen, K.; Wang, F.; Lawrence, D. S.; Zhang, Z.-Y. Probing the molecular basis for potent and selective protein-tyrosine phosphatase 1B inhibition. *J. Biol. Chem.* **2002**, *277*, 41014–41022.

(29) Chen, Y. T.; Seto, C. T. Divalent and trivalent alpha-ketocarboxylic acids as inhibitors of protein tyrosine phosphatases. *J. Med. Chem.* **2002**, *45*, 3946–3952.

(30) Chen, Y. T.; Seto, C. T. Parallel synthesis of a library of bidentate protein tyrosine phosphatase inhibitors based on the alpha-ketoacid motif. *Bioor. Med. Chem.* **2004**, *12*, 3289–3298.

(31) Xie, J.; Seto, C. T. Investigations of linker structure on the potency of a series of bidentate protein tyrosine phosphatase inhibitors. *Bioorg. Med. Chem.* **2005**, *13*, 2981–2991.

(32) Liu, G.; Xin, Z.; Pei, Z.; Hajduk, P. J.; Abad-Zapatero, C.; Hutchins, C. W.; Zhao, H.; Lubben, T. H.; Ballaron, S. J.; Haasch, D. L.; Kaszubska, W.; Rondinone, C. M.; Trevillyan, J. M.; Jirousek, M. R. Fragment screening and assembly: a highly efficient approach to a selective and cell active protein tyrosine phosphatase 1B inhibitor. *J. Med. Chem.* **2003**, *46*, 4232–4235.

(33) Comeau, A. B.; Critton, D. A.; Page, R.; Seto, C. T. A focused library of protein tyrosine phosphatase inhibitors. *J. Med. Chem.* **2010**, *53*, 6768–6772.

(34) Kolb, H. C.; Finn, M. G.; Sharpless, K. B. Click chemistry: diverse chemical function from a few good reactions. *Angew. Chem., Int. Ed.* **2001**, *40*, 2004–2021.

(35) Liu, F.; Stephen, A. G.; Fisher, R. J.; Burke, T. R., Jr. Protected aminooxyprolines for expedited library synthesis: application to Tsg101-directed proline-oxime containing peptides. *Bioorg. Med. Chem. Lett.* **2008**, *18*, 1096–1101.

(36) Liu, F.; Stephen, A. G.; Waheed A., A.; Aman, M. J.; Freed, E. O.; Fisher, R. J.; Burke, T. R., Jr. SAR by oxime-containing peptide libraries: application to Tsg101 ligand optimization. *ChemBioChem* **2008**, *9*, 2000–2004.

(37) Liu, F.; Thomas, J.; Burke, T. R., Jr. Synthesis of a homologous series of side-chain-extended orthogonally protected aminooxy-containing amino acids. *Synthesis* **2008**, 2432–2438.

(38) Liu, F.; Hakami, R. M.; Dyas, B.; Bahta, M.; Lountos, G. T.; Waugh, D. S.; Ulrich, R. G.; Burke, T. R., Jr. A rapid oxime linker-based library approach to identification of bivalent inhibitors of the *Yersinia pestis* protein-tyrosine phosphatase, YopH. *Bioor. Med. Chem. Lett.* **2010**, *20*, 2813–2816.

(39) Maly, D. J.; Choong, I. C.; Ellman, J. A. Combinatorial target-guided ligand assembly: identification of potent subtype-selective c-Src inhibitors. *Proc. Natl. Acad. Sci. U.S.A.* **2000**, *97*, 2419–2424.

(40) Jiang, Y. L.; Krosky, D. J.; Seiple, L.; Stivers, J. T. Uracil-directed ligand tethering: an efficient strategy for uracil DNA glycosylase (UNG) inhibitor development. *J. Am. Chem. Soc.* **2005**, *127*, 17412–17420.

(41) Johnson, S. M.; Petrassi, H. M.; Palaninathan, S. K.; Mohamedmohaideen, N. N.; Purkey, H. E.; Nichols, C.; Chiang, K. P.; Walkup, T.; Sacchettini, J. C.; Sharpless, K. B.; Kelly, J. W. Bisaryloxime ethers as potent inhibitors of transthyretin amyloid fibril formation. *J. Med. Chem.* **2005**, *48*, 1576–1587.

(42) Chung, S.; Parker, J. B.; Bianchet, M.; Amzel, L. M.; Stivers, J. T. Impact of linker strain and flexibility in the design of a fragment-based inhibitor. *Nat. Chem. Biol.* **2009**, *5*, 407–413.

(43) Srinivasan, R.; Uttamchandani, M.; Yao, S. Q. Rapid assembly and in situ screening of bidentate inhibitors of protein tyrosine phosphatases. *Org. Lett.* **2006**, *8*, 713–716.

(44) Tan, L. P.; Wu, H.; Yang, P. Y.; Kalesh, K. A.; Zhang, X.; Hu, M.; Srinivasan, R.; Yao, S. Q. High-throughput discovery of *Mycobacterium tuberculosis* protein tyrosine phosphatase B (MptpB) inhibitors using click chemistry. *Org. Lett.* **2009**, *11*, 5102–5105.

(45) Zhou, B.; He, Y.; Zhang, X.; Xu, J.; Luo, Y.; Wang, Y.; Franzblau, S. G.; Yang, Z.; Chan, R. J.; Liu, Y.; Zheng, J.; Zhang, Z.-Y. Targeting mycobacterium protein tyrosine phosphatase B for antituberculosis agents. *Proc. Natl. Acad. Sci. U.S.A.* **2010**, *107*, 4573–4578.

(46) Srinivasan, R.; Tan, L. P.; Wu, H.; Yang, P. Y.; Kalesh, K. A.; Yao, S. Q. High-throughput synthesis of azide libraries suitable for direct "click" chemistry and in situ screening. *Org. Biomol. Chem.* **2009**, *7*, 1821–1828.

(47) Smyth, M. S.; Ford, H., Jr.; Burke, T. R., Jr. A general method for the preparation of benzylic alpha,alpha-difluorophosphonic acids; non-hydrolyzable mimetics of phosphotyrosine. *Tetrahedron Lett.* **1992**, *33*, 4137–4140.

(48) Burke, T. R., Jr.; Kole, H. K.; Roller, P. P. Potent inhibition of insulin receptor dephosphorylation by a hexamer peptide containing the phosphotyrosyl mimetic F_2Pmp. *Biochem. Biophys. Res. Commun.* **1994**, *204*, 129–134.

(49) Yao, Z. J.; Ye, B.; Wu, X. W.; Wang, S. M.; Wu, L.; Zhang, Z. Y.; Burke, T. R., Jr. Structure-based design and synthesis of small molecule protein-tyrosine phosphatase 1B inhibitors. *Bioorg. Med. Chem.* **1998**, *6*, 1799–1810.

(50) Sun, J.-P.; Wu, L.; Fedorov, A. A.; Almo, S. C.; Zhang, Z.-Y. Crystal structure of the Yersinia protein-tyrosine phosphatase YopH complexed with a specific small molecule inhibitor. *J. Biol. Chem.* **2003**, *278*, 33392–33399.

(51) Yokomatsu, T.; Murano, T.; Suemune, K.; Shibuya, S. Facile synthesis of aryl(difluoromethyl)phosphonates through CuBr-mediated cross coupling reactions of [(diethoxyphosphinyl)difluoromethyl]zinc bromide with aryl iodides. *Tetrahedron* **1997**, *53*, 815–822.

(52) Li, Z.; Yeo, S. L.; Pallen, C. J.; Ganesan, A. Solid-phase synthesis of potential protein tyrosine phosphatase inhibitors via the Ugi four-component condensation. *Bioorg. Med. Chem. Lett.* **1998**, *8*, 2443–2446.

(53) Phan, J.; Lee, K.; Cherry, S.; Tropea, J. E.; Burke, T. R., Jr.; Waugh, D. S. High-resolution structure of the *Yersinia pestis* protein tyrosine phosphatase YopH in complex with a phosphotyrosyl mimetic-containing hexapeptide. *Biochemistry* **2003**, *42*, 13113–13121.

(54) Kolmodin, K.; Aqvist, J. The catalytic mechanism of protein tyrosine phosphatases revisited. *FEBS Lett.* **2001**, *498*, 208–213.

(55) Denu, J. M.; Dixon, J. E. Protein tyrosine phosphatases: mechanisms of catalysis and regulation. *Curr. Opin. Chem. Biol.* **1998**, *2*, 633–641.

(56) Zhang, Z.-Y. Protein-tyrosine phosphatases: biological function, structural characteristics, and mechanism of catalysis. *Crit. Rev. Biochem. Mol. Biol.* **1998**, *33*, 1–52.

(57) *ICM Chemist Pro Software*, version 3.7-1f/MacOSX; MolSoft LLC: La Jolla, CA; https://www.molsoft.com/icm-chemist-pro.html.

(58) Abagyan, R.; Orry, A.; Raush, E.; Totrov, M. *ICM User Guide 3.6*; MolSoft LLC: La Jolla, CA; https://www.molsoft.com/icm/index.html.

(59) Zhang, S.; Zhang, Z.-Y. PTP1B as a drug target: recent developments in PTP1B inhibitor discovery. *Drug Discovery Today* **2007**, *12*, 373–381.

(60) Tautz, L.; Bruckner, S.; Sareth, S.; Alonso, A.; Bogetz, J.; Bottini, N.; Pellecchia, M.; Mustelin, T. Inhibition of Yersinia tyrosine phosphatase by furanyl salicylate compounds. *J. Biol. Chem.* **2005**, *280*, 9400–9408.

(61) Feng, B. Y.; Shelat, A.; Doman, T. N.; Guy, R. K.; Shoichet, B. K. High-throughput assays for promiscuous inhibitors. *Nat. Chem. Biol.* **2005**, *1*, 146–148.

(62) Ryan, A. J.; Gray, N. M.; Lowe, P. N.; Chung, C. W. Effect of detergent on "promiscuous" inhibitors. *J. Med. Chem.* **2003**, *46*, 3448–3451.

(63) Streuli, M.; Krueger, N. X.; Hall, L. R.; Schlossman, S. F.; Saito, H. A new member of the immunoglobulin superfamily that has a cytoplasmic region homologous to the leukocyte common antigen. *J. Exp. Med.* **1988**, *168*, 1523–1530.

(64) Patterson, K. I.; Brummer, T.; O'Brien, P. M.; Daly, R. J. Dual-specificity phosphatases: critical regulators with diverse cellular targets. *Biochem. J.* **2009**, *418*, 475–489.

(65) Saikh, K. U.; Khan, A. S.; Kissner, T.; Ulrich, R. G. IL-15-induced conversion of monocytes to mature dendritic cells. *Clin. Exp. Immunol.* **2001**, *126*, 447–455.

(66) Tangy, F.; Moukkadem, M.; Vindimian, E.; Capmau, M. L.; Le Goffic, F. Mechanism of action of gentamicin components. Characteristics of their binding to *Escherichia coli* ribosomes. *Eur. J. Biochem.* **1985**, *147*, 381–386.

(67) Tropea, J. E.; Phan, J.; Waugh, D. S. Overproduction, purification, and biochemical characterization of the dual specificity H1 protein

phosphatase encoded by Variola major virus. *Protein Expression Purif* **2006**, *50*, 31–36.

(68) Lountos, G. T.; Tropea, J. E.; Cherry, S.; Waugh, D. S. Overproduction, purification and structure determination of human dual-specificity phosphatase 14. *Acta Crystallog., Sect. D* **2009**, *65*, 1013–1020.

(69) Tropea, J. E.; Cherry, S.; Nallamsetty, S.; Bignon, C.; Waugh, D. S. A generic method for the production of recombinant proteins in *Escherichia coli* using a dual hexahistidine-maltose-binding protein affinity tag. *Methods Mol. Biol. (Totowa, NJ, U. S.)* **2007**, *363*, 1–19.

(70) Welkos, S.; Pitt, M. L.; Martinez, M.; Friedlander, A.; Vogel, P.; Tammariello, R. Determination of the virulence of the pigmentation-deficient and pigmentation-/plasminogen activator-deficient strains of *Yersinia pestis* in non-human primate and mouse models of pneumonic plague. *Vaccine* **2002**, *20*, 2206–2214.

(71) Gorrec, F. The MORPHEUS protein crystallization screen. *J. Appl. Cryst.* **2009**, *42*, 1035–1042.

(72) Minor, W.; Cymborowski, M.; Otwinowski, Z.; Chruszcz, M. HKL-3000: the integration of data reduction and structure solution—from diffraction images to an initial model in minutes. *Acta Crystallogr., Sect. D: Biol. Crystallogr.* **2006**, *62*, 859–866.

(73) Vagin, A.; Teplyakov, A. Molecular replacement with MOLREP. *Acta Crystallogr., Sect. D: Biol. Crystallogr.* **2010**, *66*, 22–25.

(74) The CCP4 suite: programs for protein crystallography. *Acta Crystallogr., Sect. D: Biol. Crystallogr.* **1994**, *50*, 760−763.

(75) Murshudov, G. N.; Vagin, A. A.; Dodson, E. J. Refinement of macromolecular structures by the maximum-likelihood method. *Acta Crystallogr., Sect. D: Biol. Crystallogr.* **1997**, *53*, 240–255.

(76) Emsley, P.; Cowtan, K. Coot: model-building tools for molecular graphics. *Acta Crystallogr., Sect. D: Biol. Crystallogr.* **2004**, *60*, 2126–2132.

(77) Read, R. J. Model phases: probabilities and bias. *Methods Enzymol.* **1997**, *277*, 110–128.

(78) Schuttelkopf, A. W.; van Aalten, D. M. PRODRG: a tool for high-throughput crystallography of protein−ligand complexes. *Acta Crystallogr., Sect. D: Biol. Crystallogr.* **2004**, *60*, 1355–1363.

(79) Brunger, A. T. Free R value: a novel statistical quantity for assessing the accuracy of crystal structures. *Nature* **1992**, *355*, 472–475.

(80) Davis, I. W.; Leaver-Fay, A.; Chen, V. B.; Block, J. N.; Kapral, G. J.; Wang, X.; Murray, L. W.; Arendall, W. B., 3rd; Snoeyink, J.; Richardson, J. S.; Richardson, D. C. MolProbity: all-atom contacts and structure validation for proteins and nucleic acids. *Nucleic Acids Res.* **2007**, *35*, W375–W383.